

GAMMA/HADRON DISCRIMINATION WITH MUON IDENTIFICATION AT ARGO-YBJ.

K. FRATINI ^{a,b}, R. MEGNA ^{c,d},

^a *Dipartimento di Fisica, Università di Roma "Roma Tre", via della Vasca Navale 84, 00146 Roma, Italy*

^b *INFN, Sezione di Roma III*

^c *Dipartimento di Scienze Fisiche, Università di Napoli, Italy*

^d *INFN, Sezione di Napoli*

Abstract

Argo-YBJ (Astrophysical Radiation Ground-based Observatory at Yang-BaJing) is an air-shower particle detector array located in Tibet, at 4300 meters above sea level. It is composed of a layer of RPCs (Resistive Plate Chamber). One of its major aims is the observation of gamma-ray sources which emit from about 100 GeV up to tens of TeV. This work presents a study for the rejection of hadronic background at Argo by the use of muon identification, in order to increase its sensitivity to source detection. Thus, the introduction of a muon detector must be considered for the purpose of identifying muons. The efficiency of the technique is estimated in the case of the Crab nebula observation, which is the standard candle for gamma-ray astronomy.

1 Introduction

Argo, like all earth-based experiments, reveals air-showers, namely the products of the cascade originating from the interaction of a highly energetic primary particle (a photon or a hadron) with the nuclei composing the atmosphere. In this kind of experiments, photon detection suffers from the huge background constituted by hadronic cosmic rays.

For the purpose of observing astrophysical sources, which can often be considered as point-like objects, one has to reduce the cosmic ray background which instead is isotropically distributed. Therefore sources are surveyed within a solid angle around their direction with a suitable aperture in order to optimize the signal-to-background ratio. Thus, a good angular resolution is a fundamental task to achieve for ground-based experiments.

Background can be further reduced by exploiting the differences in shape and composition characterising photon-initiated and hadron-initiated showers. The high granularity of the Argo detector [] allows the study of detailed images of the front of the electromagnetic and hadronic showers: a hadron - photon separation algorithm based on a multifractal analysis of these images has been developed [1]. Background reduction by means of muon identification has also been investigated. This technique is based on the different muon content of the two types of shower. In this work the effectiveness of the method is tested on the Crab nebula which is the standard “candle” for this kind of investigations: the quality factor and the sensitivity to the Crab nebula have been estimated.

2 The quality factor Q

The background rejection efficiency can be estimated by means of the quality factor Q ,

$$Q = \frac{\epsilon_\gamma}{\sqrt{1 - \epsilon_B}} \quad (1)$$

where ϵ_γ and ϵ_B are respectively the γ identification efficiency (the fraction of showers generated by photons and recognised as such) and the background identification efficiency (the fraction of showers generated by hadrons and recognised as such). Indeed Q is the factor by which the sensitivity to a certain source increases when some background rejection technique is applied with respect to the case of no rejection. In fact, the sensitivity is,

$$S_Q = \frac{N_\gamma \cdot \epsilon_\gamma}{\sqrt{N_B \cdot (1 - \epsilon_B)}} = \frac{N_\gamma}{\sqrt{N_B}} \cdot Q \quad (2)$$

where N_γ and N_B are the number of photons and hadrons detected without any background identification, ϵ_γ and ϵ_B have just been defined. Thus, the numerator represents the overall number of photons identified with the chosen technique, while the denominator is the statistical fluctuation of the number of background events which are left after the identification.

The quality factor Q depends on the energy of the primary particles hitting the atmosphere. Its behaviour as a function of the energy must be determined. In this work both the Q factor and the sensitivity to the Crab nebula as a function of the minimum pad¹ multiplicity and median energy are calculated.

¹“Pad” is the logical unit used in the Argo setup, consisting in a square of about 56×62 cm². The pad multiplicity is one of the observables which the Argo detector can measure. However, the pad multiplicity is correlated to the energy of primary particles. In this work the median energy related to the multiplicity bins considered has been estimated. Thus physical quantities are expressed as a function of the pad multiplicity and median energy.

3 Upgrade of the Argo detector

The standard configuration of the detector includes a central “carpet” surrounded by a ring (Fig. 1, left). As already stated, the introduction of muon identification requires an upgrade to this configuration. Because of the high energies involved, a detector layout with a larger number of active elements (RPCs) has been considered in this work, in order to enlarge the sensitive area: the empty space between the carpet and the ring, and between the elements of the ring itself has been filled with RPCs, thus obtaining the configuration shown in Fig. 1, right.

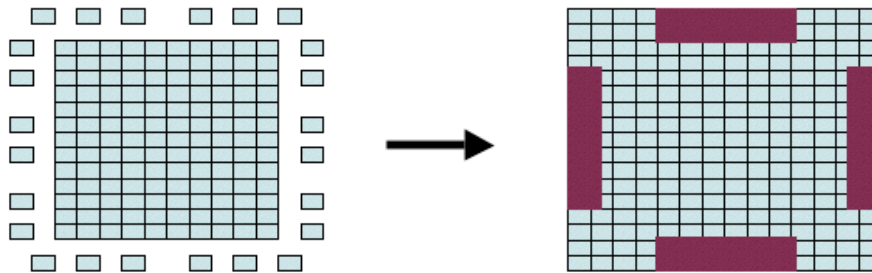


Figure 1: *The standard configuration of the Argo detector (left) and the proposed upgraded configuration (right). The light squares represent clusters of RPCs, the dark rectangles the muon trackers.*

The next change to introduce is the addition of a muon tracker. It is typically constituted of few tracker layers interspersed with an absorber. Apart from the kind of detector that can be chosen, some very general constraints have been imposed:

- muon energy detection threshold equal to 1 GeV which corresponds to a concrete layer about 2 m thick;
- two values for the total muon detection area has been considered: 1500 m² and 2500 m².

The results reported in this work assume that the muon detector efficiency, in the energy range of interest, is 100%.

4 Evaluation of the Q factor.

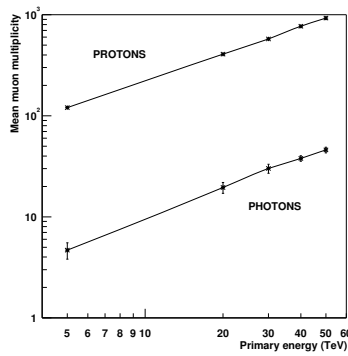
The sample of events used in this work was generated by means of the simulation program *Corsika*. The software was modified in order to simulate photons coming from the Crab nebula during its trail in the sky. As far as the background simulation is concerned, the cosmic ray spectrum has been supposed to be composed

only by protons. The helium component has been taken into account by properly increasing the number of simulated protons.

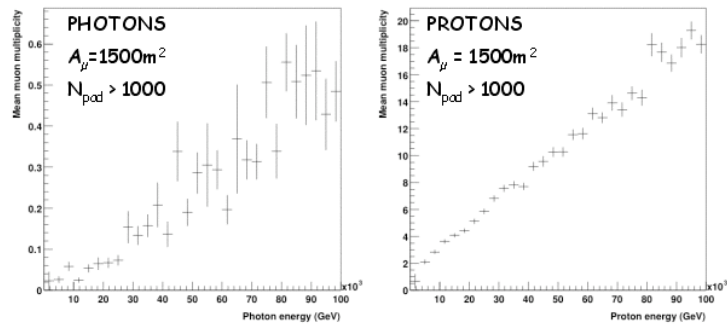
The interaction of the shower products with the detector was simulated by a *Geant*-based code developed by the collaboration. The standard event reconstruction was then applied.

4.1 The air-shower muon content.

As shown in Fig. 2a, the number of muons contained in vertical air-showers rises as a function of the energy of the primary particle both for protons and photons. However, the muon content of photon-initiated showers is two orders of magnitude lower than the proton-generated one. Therefore, the number of muons present in a certain event can be used as a discriminating variable between photon-induced and hadron-induced showers. The number of muons has also been estimated in



[a]



[b]

Figure 2: The mean number of muons for vertical proton-induced and photon-induced air-showers as a function of the primary energy.

the case of the simulated observation of the Crab nebula. Indeed, Fig. 2b shows the mean muon content as a function of the primary energy in the reconstructed events detected by Argo: photon-initiated showers are almost lacking in muons. The muon detection technique is expected to be more efficient at high energy (tens of TeV).

4.2 Method and results.

The method used to calculate the identification efficiencies ϵ_γ and ϵ_B is straightforward. The distributions of the number of muons per event relative to photon- and proton-generated showers are obtained. Events are then identified as photon or proton type, based on a cut on the number of muons. If, for example, the cut

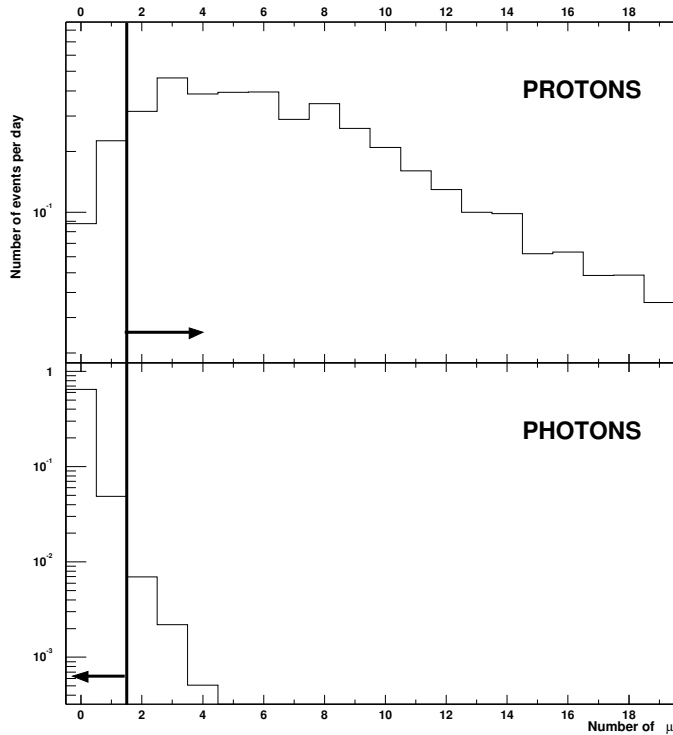


Figure 3: The distribution of the number of muons per event, detected with the apparatus described in Section 3 for proton-initiated (above) and photon-initiated (below) showers. The area on the right (left) side of the vertical line representing the cut value is equivalent to the number of protons (photons) identified as such.

value is set at two muons, then an event containing two or more revealed muons

will be tagged as a proton-generated shower, otherwise as a photon-generated one. Figure 3 shows the distribution of the number of muons for both protons (above)

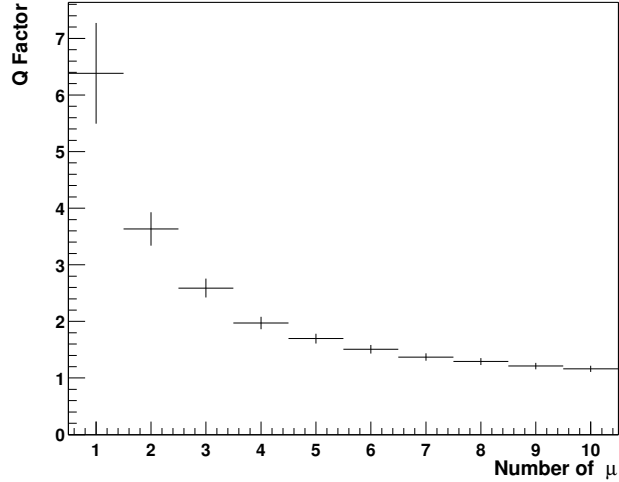


Figure 4: Q versus muon number for minimum pad multiplicity equal to 2000.

and photons (below). The cut value is indicated by the vertical line: protons on the right side of the line are identified as such, photons on the left side of the same line are identified as such. Now the Q factor can be calculated using Eq. 1. Different values are obtained as a function of different cuts set on the muon multiplicity: this is shown in Fig. 4 in a particular configuration (number of hit pad larger than 2000 and muon detection area equal to about 1500 m²). For lower values of the cut the Q factor is higher because a greater number of protons can be identified and the number of photons tagged as protons and therefore rejected is not significant.

The Q factor as a function of the median energy is shown for different values of the discriminating muon number in Fig. 5 in the case of a muon detection surface of 1500 m². Its rise with the energy is due to the fact that at higher energy the average number of muons present in proton-initiated air-showers increases, thus allowing a better discrimination between signal and background. This estimate of the background rejection power has been performed applying the conditions subsequently described in Sec. 5 when calculating the sensitivity to the Crab nebula.

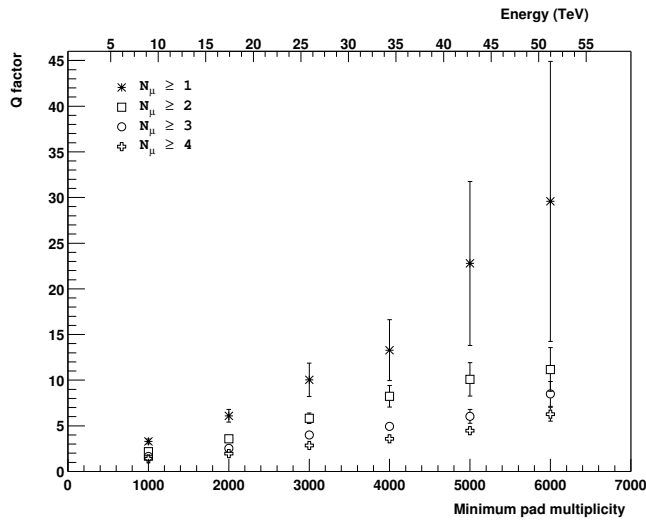


Figure 5: Q factor as a function of the minimum pad multiplicity and the median energy for different values of the number of muons N_μ chosen to discriminate among the electromagnetic and hadronic showers in the case of a muon detection surface of 1500 m^2

5 Sensitivity to the Crab nebula

In the Argo usual configuration, the expected sensitivity to the Crab nebula has already been calculated in [2] at energies up to TeV. Here, the active area has been increased in such a way as to detect the maximum number of photons allowed at present. The conditions applied to estimate the Argo sensitivity to the “standard candle” has also been chosen with the purpose of maximising the number of detected events. The estimate of the sensitivity has been evaluated at higher energies, under the following assumptions:

- The Crab nebula spectrum simulated is the one measured by the Whipple collaboration [3]:

$$\frac{dN}{dE} = 3.2 \cdot 10^{-7} E^{-2.49} \gamma \text{ m}^{-2} \text{ s}^{-1} \text{ TeV}^{-1} \quad (3)$$

- The simulated proton flux on the top of the atmosphere is [4]:

$$\frac{dN}{dE} = 8.98 \cdot 10^{-2} E^{-2.74} \text{ p m}^{-2} \text{ s}^{-1} \text{ sr}^{-1} \text{ TeV}^{-1} \quad (4)$$

- Only events whose reconstructed core falls inside the “fiducial area” $A_f = 107 \times 95 \text{ m}^2$ and with the reconstructed zenith angle $\theta \leq 40^\circ$ are selected.

- For high values of pad multiplicity, the observational opening angle is 0.29° [2]

The integrated sensitivity as a function of the minimum pad multiplicity and the median energy with the enlarged detection area is plotted in Fig. 6. The error bars stand for the statistical error. This estimate of the sensitivity does not exploit the background rejection achievable thanks to the muon identification while Fig. 7a shows the expected sensitivity as a function of the minimum pad multiplicity and the median energy when making use of this discrimination technique in the case of a detection surface of 1500 m^2 , for different values of the muon number N_μ chosen to tag the events. Figure 7b shows again this sensitivity together with the

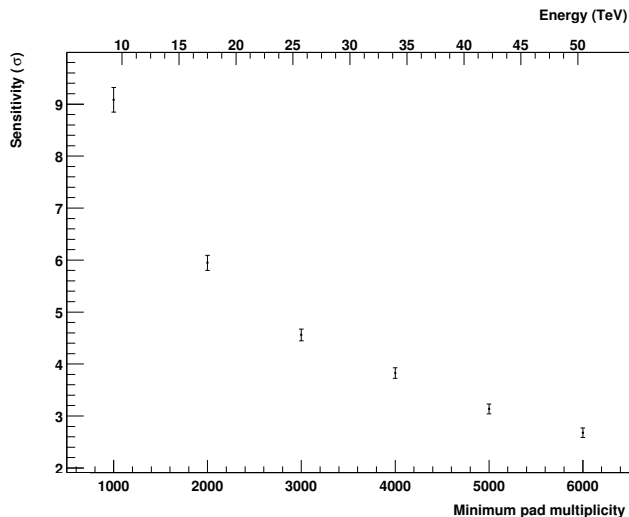
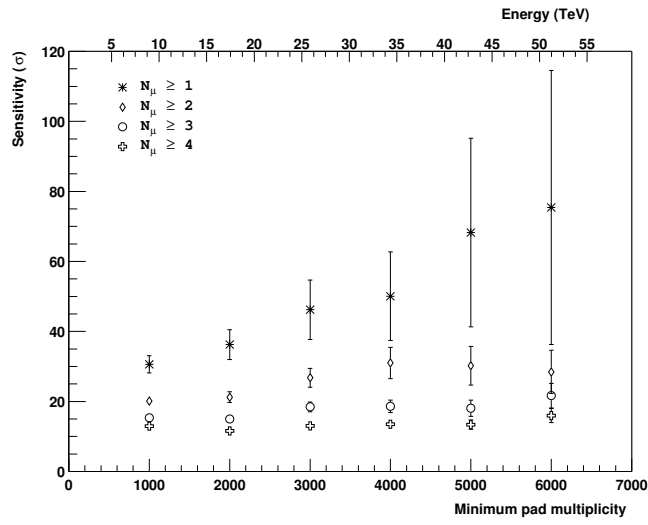


Figure 6: *Sensitivity as a function of the minimum pad multiplicity and median energy with the enlarged active detector surface, without muon identification.*

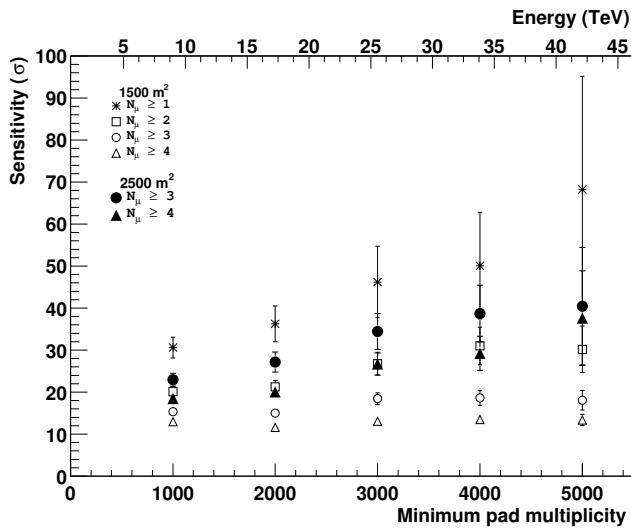
sensitivity estimated in the case of 2500 m^2 detection surface, setting the value of the discriminating number of muons N_μ to 3 and 4. The sensitivity obtained in this second experimental configuration is higher for equal values of N_μ . In particular the results showed in Fig. 7b are in between those obtained using 1500 m^2 of muon detector with N_μ equal to 1 and 2.

6 Study of the Crab spectrum at high energy

The background reduction achieved by means of the muon identification method is rather high. Thus, the study of the Crab spectrum at the highest energies can be faced. In particular, the ability of the Argo experiment to distinguish among two



[a]



[b]

Figure 7: Sensitivity as a function of the minimum pad multiplicity and the median energy with the enlarged active detector surface and with a muon detector of 1500 m^2 . N_μ is the number of muons used to discriminate among the electromagnetic and hadronic showers (a). The sensitivity with a muon detector of 2500 m^2 is superimposed in the case of discriminating muon numbers equal to 3 and 4 (b).

different behaviours of the Crab spectrum has been examined in the case of a muon detector surface of 1500 m². Two hypothetical scenarios have been considered:

- the energy spectrum has a cutoff at 40 TeV;
- the energy spectrum has a cutoff at 70 TeV.

The aim is to understand if these two situations can be separated with the help of the muon identification technique. The study has been performed on simulated data corresponding to three years of data taking. Figure 8 shows the total number of proton- and photon-initiated air-showers before (points above) and after (point below) rejecting those containing 2 or more muons, as a function of the minimum pad multiplicity, in the two cases above. The two scenarios are best separated at high values of the minimum pad multiplicity. The estimate has been performed with the conditions described in the previous Section.

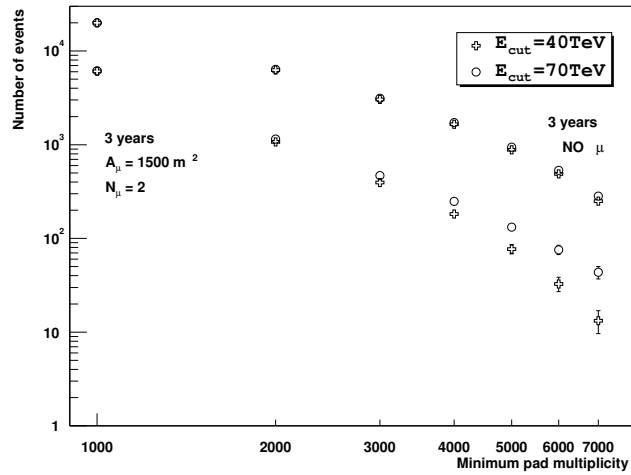


Figure 8: Q vs. number of muons.

References

- [1] I. Demitri, - these proceedings, (2004)
- [2] S. Vernetto *et al*, Proc XXVII ICRC, (2003).
- [3] A. M. Hillas et al. *ApJ* 503, 744 (1998)

-
- [4] T.K. Gaisser et al. *Proc XXVII ICRC*, 1643 (2001)
- [5] L. Lamport, *L^AT_EX - A Document Preparation System - User's Guide and Reference Manual*, Addison-Wesley, Reading (1985)
M. Goossens, F. Mittelbach, A. Samarin. *The L^AT_EX Companion*, Addison-Wesley, Reading (1994)
T. Oetiker, H. Partl, I. Hyna, E. Schegl, *The Not So Short Introduction to L^AT_EX 2_ε*,
<http://people.ee.ethz.ch/~oetiker/lshort/lshort.pdf> (2003)